SUPPLEMENTARY INFORMATION

Methods

Adeno-associated virus production and transduction. The pAAV-CaMKIIα-ChR2(H134R)-EYFP plasmid was constructed by cloning CaMKIIα-ChR2(H134R)-EYFP into an AAV backbone using MluI and EcoRI restriction sites. The maps are available online at www.optogenetics.org. The recombinant AAV vectors were serotyped with AAV5 coat proteins and packaged by the viral vector core at the University of North Carolina; titers were $2x10^{12}$ particles/mL for both viruses.

Immunohistochemistry and imaging. To verify the phenotype of cells, rodents were anaesthetized with 65 mg/kg sodium pentobarbital and transcardially perfused with ice-cold 4 % paraformaldehyde (PFA) in PBS (pH 7.4). Brains were fixed overnight in 4 % PFA and then equilibrated in 30% sucrose in PBS. 40 µm-thick coronal sections were cut on a freezing microtome and stored in cryoprotectant (25 % glycerol, 30 % ethylene glycol, in PBS) at 4ºC until processed for immunohistochemistry. Free-floating sections were washed in PBS and then incubated for 30 min in 0.2 % Triton X-100 (Tx100) and 2 % normal donkey serum (NDS). Slices were incubated overnight with primary antibody in 2 % NDS (Mouse anti-CaMKIIα 1:500, Abcam, Cambridge, MA; Mouse anti-Parvalbumin 1:500, Sigma, St Louis, MO; Rabbit anti-GABA 1:500, Millipore, Billerica, MA; Chicken anti-GFAP 1:250, Millipore; Mouse anti-MAP2 1:500, Sigma). Sections were then washed with PBS and incubated for 2hr at RT with secondary antibodies (Donkey anti-Mouse conjugated to either Cy3 or FITC, donkey anti-Rabbit Cy5 and donkey-anti chicken Cy5, all 1:1000, Jackson Laboratories, West Grove, PA). Slices were then washed, incubated with DAPI (1:50,000) for 20 min, washed again, and mounted on slides with PVA-Dabco (Sigma). Confocal fluorescence images were acquired on a scanning laser microscope using a 20X/0.70NA or a 40X/1.25NA oil immersion objective.

Stereotactic injection and cannula placement. Female adult (>10 weeks old) Fischer and Sprague-Dawley (250-350 g) rats were the subjects; animal husbandry and all aspects of experimental manipulation were in strict accord with guidelines from the National Institute of

Health and have been approved by members of the Stanford Institutional Animal Care and Use Committee (IACUC). Rats were anaesthetized using 1.5 % isoflurane (for surgeries longer than 1 hr) or i.p. injection (90 mg/kg ketamine and 5mg/kg xylazine). The top of the animal's head was shaved, cleaned with 70 % ethanol and betadine and then positioned in the stereotactic frame. Ophthalmic ointment was applied, a midline scalp incision was made, and small craniotomies were performed using a drill mounted on the frame. Four types of surgeries were conducted: **I)** viral injection (1 µl/site) and cannula (1.5 mm projection) placement in M1 (+ 2.7 mm AP, + 3.0 mm ML right hemisphere, two injections at - 2.0 and - 2.5 mm DV); **II)** 4 viral injections across cortex (1: + 5. 2 mm AP, + 2.0 mm ML right hemisphere, one 2 µl injection at -3.0 DV; 2: + 3.2 mm AP, + 3.5 mm ML right hemisphere, 3 injections each 0.7 µl at -3.5 mm, -3.0 mm, and -2.5 mm DV; 3: + 2.7 mm AP; + 0.5 mm ML right hemisphere; 2 injections 1 µl each at - 3.0 mm and - 2.5 mm DV; 4: - 0.3 mm AP; + 3.0 mm ML right hemisphere; 2 injections 1 µl each at -2.5 mm and - 2.0 mm DV; and the cannula (6.5 mm projection) was placed in ventral thalamus at the border with ZI (- 4.3 mm AP; + 2 mm ML right hemisphere; -6.5 mm DV); **III)** viral injection (1 µl/site) and cannula (5.25 mm projection) placement in thalamus (+ 2.7 mm AP, + 3.0 mm ML right hemisphere, two injections at - 5.25 and - 5.75 mm DV). **IV)** Doublefloxed inverted-open reading frame (DIO) ChR2-EYFP was injected stereotactically into the motor cortex (2.0 mm AP; 1.42 mm ML, two injections at -1.25 mm and -1.75 mm DV) of 5-10-week-old transgenic mice expressing Cre recombinase in fast-spiking parvalbumin-expressing GABAergic interneurons (*PV::Cre*)[1,2,3].

Concentrated virus was delivered using a 10 µl syringe and a thin 34 gauge metal needle; injection volume and flow rate (0.1 µl/min) were controlled with an injection pump. After the final injection, the needle was left in place for 5 additional minutes and then slowly withdrawn. An MRI compatible cannula fiber guide (8IC313GPKXXC) was inserted through the craniotomy. One layer of adhesive cement followed by cranioplastic cement was used to secure the fiber guide system to the skull. After 10 min, the scalp was sealed using tissue adhesive. The animal

was kept on a heating pad during recovery from anesthesia. Buprenorphine (0.03 mg/kg) was given subcutaneously following the surgical procedure to minimize discomfort. A dummy cannula (8IC312DCSPCC) was inserted to keep the fiber guide patent.

To avoid scanning animals with damage associated with the cannula implantation, detailed anatomical MRI scans were performed to check for tissue damage. In cases where damage near the cannula was detected in the T_2 weighted high-resolution anatomical images, animals were rejected and not used in experiments. Moreover, animals used for fMRI studies were examined post-mortem for local invasion and for gliosis, using DAPI and GFAP staining (GFAP is a sensitive marker for gliosis and can report changes in local glial number, glial activation, and inflammation). In all subjects used for fMRI, we did not see evidence for cellular invasion or for gliotic changes (Supplementary Figure 1) beyond the expected 30-50 μm from the cannula, indicating that the boundaries of the BOLD responses are not determined by local damage or gliosis under these conditions.

fMRI. fMRI scans were conducted with a small animal dedicated MRI scanner, custom designed pulse sequences, RF coils, and cradle. The small animal scanner consisted of a Magnex scientific superconducting magnet with 7.0 Tesla (T) field strength, RRI gradient with clear bore size of 9 cm, maximum gradient amplitude of 770 mT/m and maximum slew rate of 2500 T/m/s and a General Electric (GE) console and radiofrequency (RF) amplifiers with maximum RF amplitude of 24.7 μT. The animals were first anesthetized in a knockdown box with 4% isoflurane. After approximately 5 minutes in the knockdown box, the animal was intubated, placed on a custom-designed MRI-compatible cradle with a stereotaxic frame, and the tracheal tube connected to a ventilator (Harvard Apparatus, Model 683 Small Animal Ventilator) with 1.3-1.5 % isoflurane, 35 % O_2, 65% N_2O input gas and a capnometer (SurgiVet V9004). A 3.5 cm diameter custom-designed transmit/receive single-loop surface coil was placed on the top of the target, and a 300 μm diameter optical fiber was then inserted through the guide. A fiber-optic

rectal temperature probe was inserted and the cradle with the animal was inserted to the iso-center of the magnet. Expiratory CO_2 content was continuously monitored by a capnometer. The ventilation volume and frequency (3.0-3.5 cc/stroke, 50-60 stroke/min) was controlled to keep the endtidal CO_2 level at ~3.5 % throughout the scan. Heated air was pumped into the bore to maintain animal's body temperature at physiological levels (34-38 ^{o}C).

fMRI scans were performed using conventional GRE-BOLD fMRI methods and passband b-SSFP fMRI[4] methods. Passband bSSFP-fMRI was designed to be a 3D volumetric, b-SSFP sequence with stack-of-spirals[5] readout trajectory. To get good slab selection for the passband bSSFP-fMRI scans, a time-bandwidth (TBW) of 12 pulse was designed with a duration of 1 ms. 10 interleave in-plane spirals with 32 stack locations, 9.372 ms T_R, 2 ms T_E resulted in 30 slices (2 slices discarded due to 3D slice direction excitation profile roll-off margin) and 1.5 cm slice direction volume coverage.

fMRI data was first reconstructed through a 2-dimensional (2D) and 3D gridding reconstruction methods. The reconstructed 4D magnitude image data was then analyzed by calculating the individual voxel coherence value (c)[6], defined as the magnitude of the frequency component of interest ($|F(f_0)|$) divided by the sum-of-squares of all frequency components ($\sqrt{\sum_f |F(f)|^2}$; F: Fourier transform of temporal signal intensity; f_0: frequency of stimulation— here, $\frac{1}{60}$ Hz). Therefore, the coherence value (c) is between 0 and 1. The coherence value was thresholded at 0.35, color coded and overlaid onto *T_2* anatomical images.

$$c = \frac{|F(f_0)|}{\sqrt{\sum_f |F(f)|^2}}$$

Coherence values (c) can be converted to z- and p-values given the mean (m), variance (σ^2) of the null-hypotheses distribution. The following formula can be used to calculate the corresponding z value given the c value, m, σ, and N (sample size for estimation of m and σ).

$$z = \frac{1}{\sigma}\left(\sqrt{\frac{c^2}{(1-c^2)}((N-1)\sigma^2 + Nm^2)} - m\right)$$

The p-value can then be estimated with an assumption for the null-hypothesis. For example, in our study, coherence of 0.35 corresponds to z-value of approximately 4.6, which gives a p-value of approximately 0.000002 when Gaussian distribution is assumed. Therefore, the p-value threshold in all our experiments can be assumed to be less than 0.001. For most of the data, the thresholded coherence value was overlaid onto T_2 anatomical images to show "activated" voxels. However, for the PV::Cre stimulation result, since pixels with opposite phase with respect to stimulation were present, color-coded phase values of pixels with coherence level over 0.35 were displayed to show the distribution of *positive* and *negative* BOLD. The phase value (θ) was calculated as the phase of the frequency component of interest, resulting in phase values between 0 and 2π (0 corresponds to no delay with respect to stimulus, and π corresponds to the half cycle delay of 30 s in these experiments).

$$\theta = \angle(F(f_0))$$

Voxel-based frequency analysis was used as the method with fewest assumptions instead of model-based methods since the HRF of ofMRI was not known.

In vivo optrode recordings. Simultaneous optical stimulation and electrical recording in living rodents was conducted as described previously using an optrode composed of an extracellular tungsten electrode (1 MΩ, ~125 μm) attached to an optical fiber (~200 μm) with the tip of the electrode deeper (~0.4 mm) than the tip of the fiber to ensure illumination of the recorded neurons. For stimulation and recording in two distinct regions (M1 and thalamus), small craniotomies were created above both target regions. The optical fiber was coupled to a 473 nm laser diode from CrystaLaser. Optrode recordings were conducted in rats anesthetized with 1.5% isoflurane. pClamp 10 and a Digidata 1322A board were used to both collect data and generate light pulses through the fiber. The recorded signal was bandpass filtered at 300Hz low/5 kHz high (1800 Microelectrode AC Amplifier) and filtered in Clampfit to remove 60 Hz

noise. For precise placement of the fiber/electrode pair, stereotactic instrumentation was used.

Opsin expression validation. Acute coronal brain slices (250 μm) were cut by vibratome, and slices were fixed for 1hr in 4% paraformaldehyde, washed with PBS, mounted on microscope slides, and examined by confocal microscopy at high and low magnification to observe both opsin localization and cannula placement. Confocal fluorescence images were acquired on a scanning laser microscope using a 20X/0.70NA or a 40X/1.25NA oil immersion objective, while large field images of entire slices were collected on a Leica MZ16FA stereomicroscope.

In vivo Optical Stimulation. 20 Hz, 15 ms pulsewidth stimulation with 473 nm light was used for all fMRI and optrode recordings. 300 μm diameter optical fibers were used with the optical fiber output power level at approximately 6 mW. These power levels correspond to 85 mW mm^{-2} at the fiber output, but more than 10-fold less over the majority of the excitation volume given the expected light scattering profile[7]. Assuming 1 mW/mm^2 is the minimum light power needed to activate ChR2, the light penetration depth of direct light activation is expected to be ~0.95 mm[7]. Optical stimulation power must be set with care in order to avoid potential BOLD signal confound due to heating; we have found that at higher laser power levels or with steady illumination, laser synchronized signal intensity change can be observed even in control animals; the BOLD sequence, which gives T_2*-weighting has been found to have no significant temperature dependence at lower temperatures, while high enough temperature causing tissue damage has been found to result in signal amplitude decrease[8]. We therefore, chose to use <=~6 mW of laser power and maintained pulsed waveforms with 30% duty cycle.

Analysis of Electrophysiological Data. Threshold search in Clampfit was used for automated detection of spikes in multi-unit recording, which was then validated by visual inspection. For traces with multiple spike populations, thresholds were set to capture all the spikes; during bursting, it is likely that multiple neurons were recorded from simultaneously.

REFERENCES

1 Cauli, B. *et al.*, Cortical GABA Interneurons in Neurovascular Coupling: Relays for Subcortical Vasoactive Pathways. *Journal of Neuroscience* 24 (41), 8940-8949 (2004).

2 Cardin, J.A. *et al.*, Driving fast-spiking cells induces gamma rhythm and controls sensory responses. *Nature* 459 (7247), 663-667 (2009).

3 Sohal, V.S., Zhang, F., Yizhar, O., & Deisseroth, K., Parvalbumin neurons and gamma rhythms enhance cortical circuit performance. *Nature* 459 (7247), 698-702 (2009).

4 Lee, J.H. *et al.*, Full-brain coverage and high-resolution imaging capabilities of passband b-SSFP fMRI at 3T. *Magn Reson Med* 59 (5), 1099-1110 (2008).

5 Lee, J.H., Hargreaves, B.A., Hu, B.S., & Nishimura, D.G., Fast 3D imaging using variable-density spiral trajectories with applications to limb perfusion. *Magn Reson Med* 50 (6), 1276-1285 (2003).

6 Engel, S.A., Glover, G.H., & Wandell, B.A., Retinotopic organization in human visual cortex and the spatial precision of functional MRI. *Cereb Cortex* 7 (2), 181-192 (1997).

7 Aravanis, A.M. *et al.*, An optical neural interface: in vivo control of rodent motor cortex with integrated fiberoptic and optogenetic technology. *J Neural Eng* 4 (3), S143-156 (2007).

8 Parker, D.L., Applications of NMR imaging in Hyperthemia: An evaluation of the Potential for Localized Tissue Heating and Noninvasive Temperature Monitoring. *IEEE TRANSACTIONS ON BIOMEDICAL ENGINEERING* BME-31 (1), 161-167 (1984).

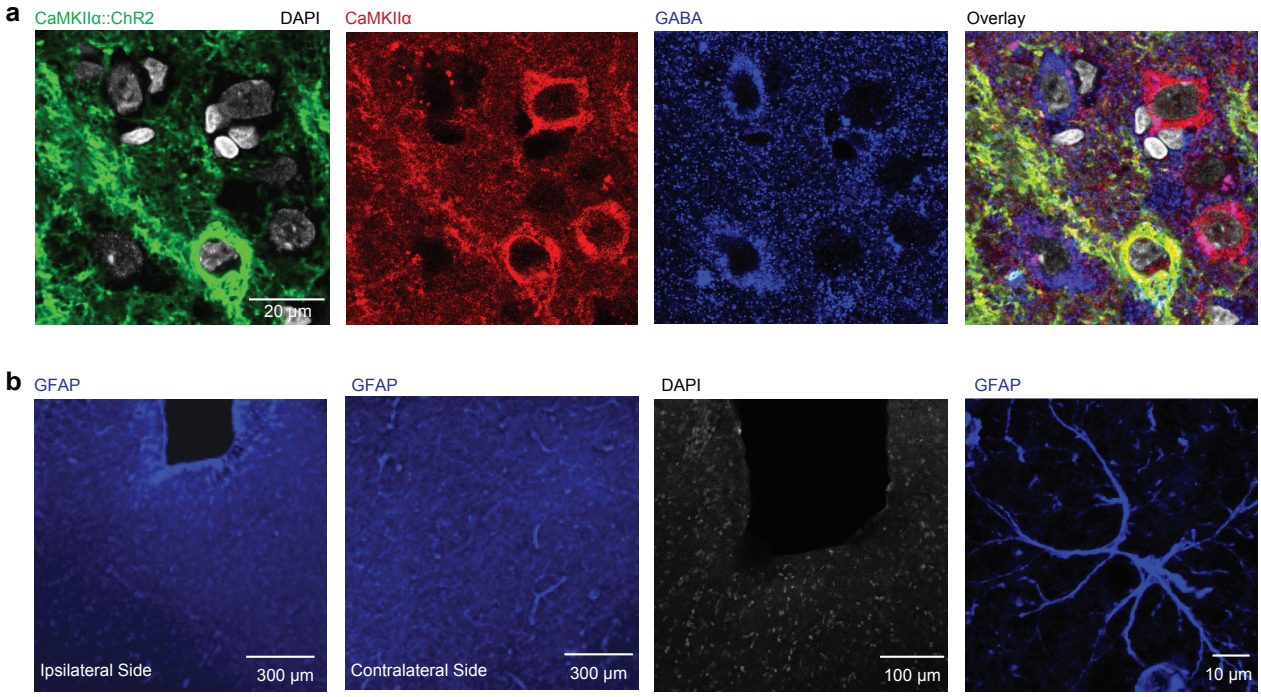

Figure S1. Histological characterization of CaMKIIα specificity, efficacy and transduction region. a, AAV5-CaMKIIα::ChR2-EYFP: Costaining for the excitatory marker CaMKIIα, inhibitory maker GABA and nuclear marker DAPI. Overlay of EYFP, CaMKIIα, GABA and DAPI reveals colocalization of YFP and CaMKIIα in the cell body. Cells expressing GABA are present but do not coexpress EYFP. Regarding specificity, 99% of cells expressing EYFP (photosensitive) were positive for CaMKIIα (167/169 cells; 2/169 were positive for GABA). Regarding transduction efficacy, 89% (231/259) of all CaMKIIα cells counted were EYFP positive in the opsin expression region of 6.4 mm^3. **b,** Costaining for the nuclear marker DAPI and astroglial marker GFAP showing that BOLD signal boundaries do not map onto gliosis, which accounted for only the expected thin <30-50 μm rim around the implantation site. GFAP staining was similar on injected and non-injected hemispheres; high-magnification view of GFAP staining shown at right.

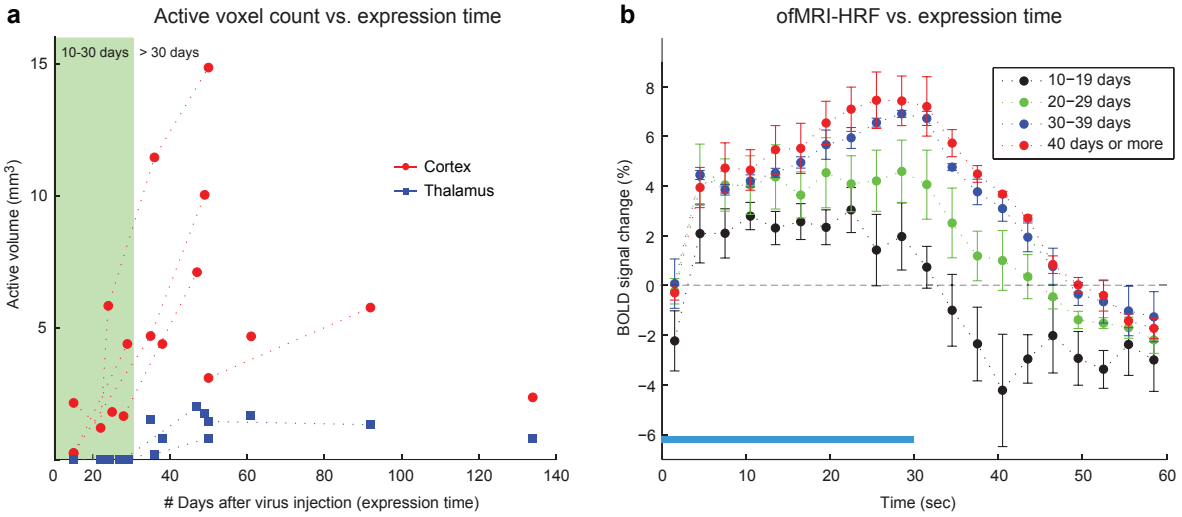

Figure S2. Optically-induced BOLD signals and ChR2-EYFP expression. a, Volume of active voxels in M1 (red) and thalamus (blue) plotted as a function of days post-injection with CaMKIIα::ChR2-EYFP. Dotted lines link serially acquired data from the same animal. Animals with less than 30 days of expression time showed smaller activated volume in cortex and thalamus. **b**, ofMRI-HRFs in animals expressing <30 d reached plateau at 5 s, in contrast to ofMRI-HRFs in animals expressing >30 d.

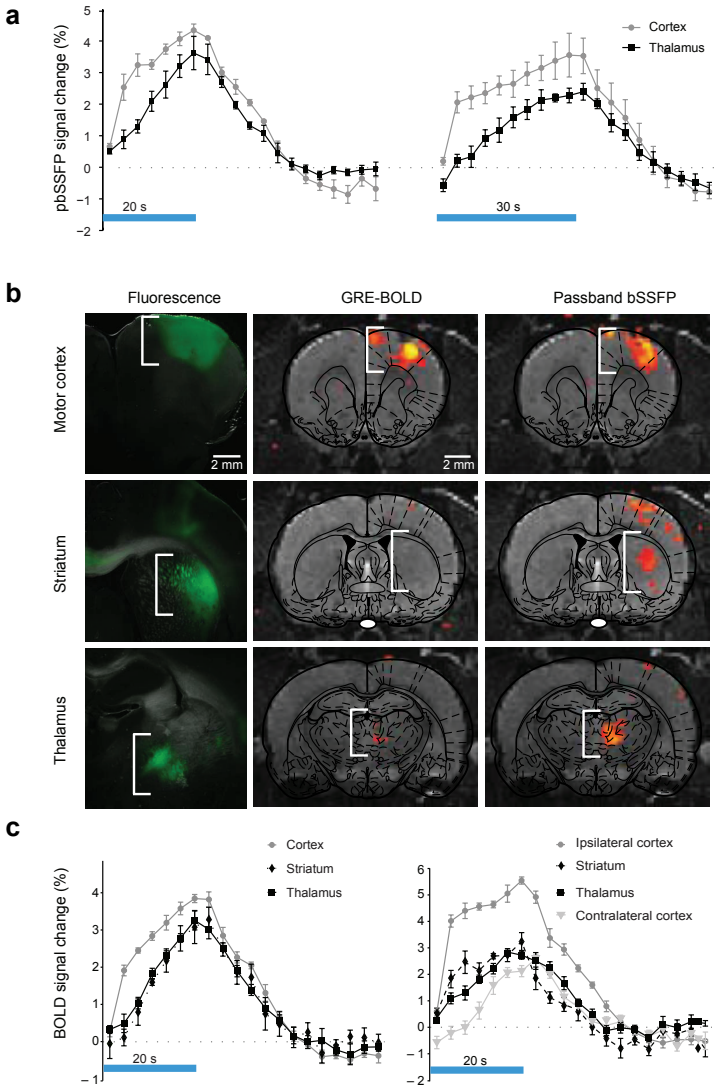

Figure S3. ofMRI circuit mapping: conventional BOLD and passband bSSFP-fMRI. a, Passband b-SSFP ofMRI-HRF[4]; 20 s (n=3), 30 s (n=6). The passband b-SSFP ofMRI-HRF shows the same temporal character as conventional GRE-BOLD. **b,** Injection of CaMKIIα::ChR2-EYFP in M1, as expected, leads to opsin visualization in motor cortex, striatum, and thalamus, i.e. the primary site of injection and sites where axons of expressing neurons extend. Middle column: hemodynamic response following M1 stimulation: conventional BOLD fMRI superimposed onto appropriate atlas image. Right column: Imaging the same hemodynamic response with passband bSSFP-fMRI[4], which more fully captures circuit-level activity. **c,** ofMRI-HRF from two representative animals that showed activity in motor cortex, striatum, contral-lateral motor cortex, and thalamus. For the HRF plotted on the left, activation volume for motor cortex was 11.3 mm^3, striatum was 2.9 mm^3, thalamus was 2.9 mm^3. For the HRF plotted on the right, activation volume for motor cortex was 12.1 mm^3, striatum was 1.5 mm^3, thalamus was 1.3 mm^3, and contralateral cortex was 1.4 mm^3.

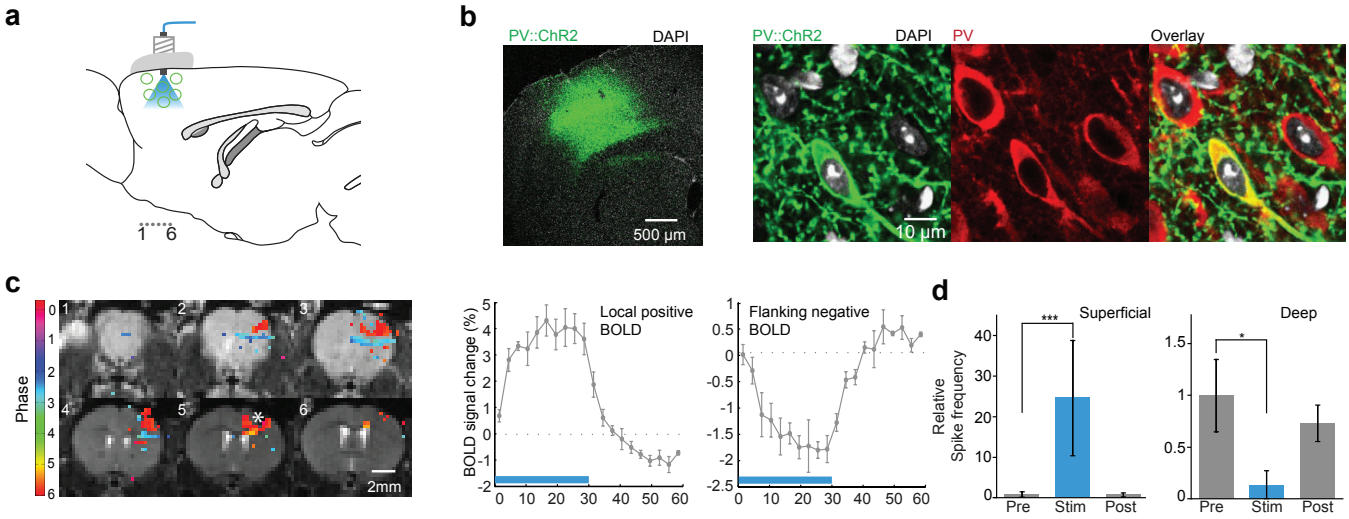

Figure S4. ofMRI and fast-spiking inhibitory interneurons: local positive and flanking negative BOLD. Doublefloxed inverted open-reading-frame (DIO; Cre-dependent) ChR2-EYFP AAV was stereotactically injected into the motor cortex of transgenic mice expressing Cre recombinase in parvalbumin-expressing cells (PV::Cre)[1,2,3]. **a,** Schematic: Cre-dependent ChR2-EYFP was injected into cortex with optical stimulation at the same location. Coronal imaging slices shown in (c) marked as "1..6". Transduced cells (circles) and blue light delivery are shown at cannula implantation and stimulation site. **b,** Immunohistochemistry demonstrating ChR2-EYFP expression in PV positive cell bodies. 98.5% (263/267) of ChR2-EYFP expressing cells were also PV positive and 72.7% (263/362) of PV positive cells expressed ChR2-EYFP. The opsin expression region was ~3.0 mm^3. **c,** BOLD ofMRI coherence-thresholded phase map (20Hz stimulation) shows positive BOLD in the close vicinity of the optical stimulation with flanking negative BOLD, consistent with local optogenetic excitation of these cells and lateral inhibitory properties[1,2,3]; as before, asterisk indicates injection site and fiber termination/stimulation site. Also shown are summary graphs for positive BOLD ofMRI-HRF (n=3) (*left*) and negative BOLD ofMRI-HRF (n=3) (*right*). Mean volume was 1.7±0.7 mm^3 for positive BOLD and 0.6±0.6 mm^3 for negative BOLD. **d,** Extracellular optrode recordings during 473 nm optical stimulation (20 Hz/15 ms pulsewidth) revealing both excitation (superficial) and inhibition (deep) in cortex. Excitation was observed superficially with a standard optrode, while inhibition was observed with an optrode constructed with electrode tip 0.76 µm deeper relative to the optical fiber tip than with the standard optrode. Spike rate normalized to baseline increased locally (two-sample t-test; $p<0.001$; n=14) during excitation, consistent with 20 Hz optical drive of the targeted cells, and decreased distally during inhibition (two-sample t-test; $p<0.05$; n=4).

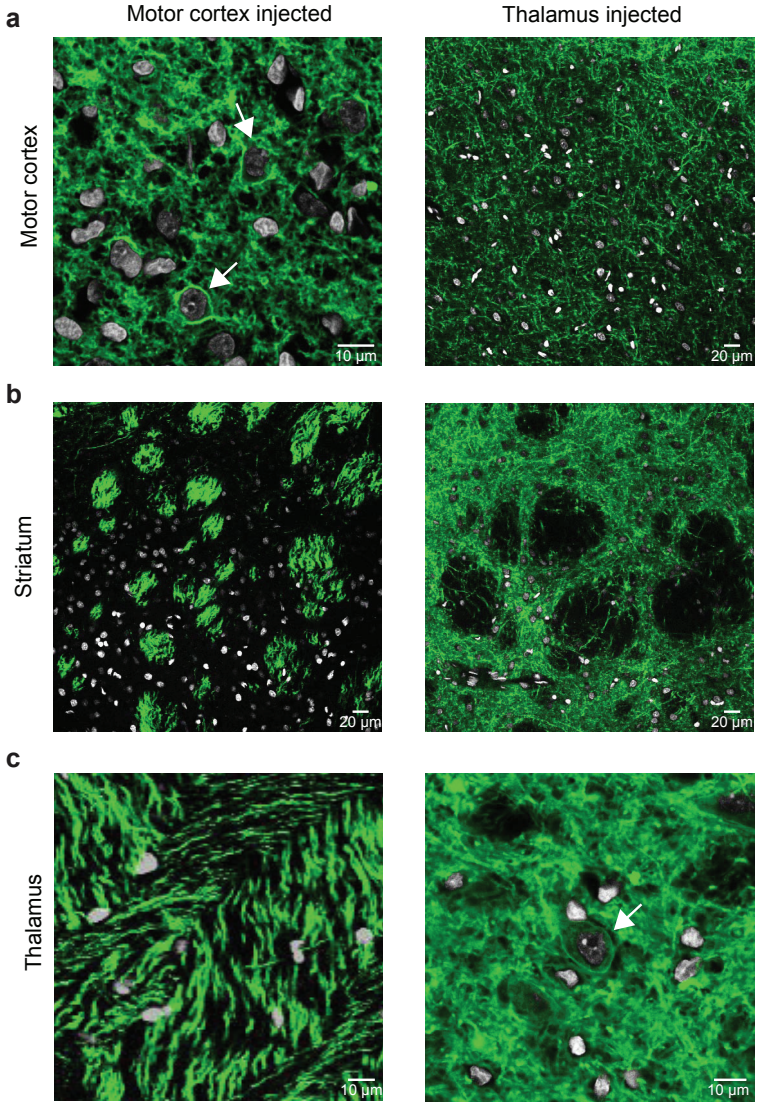

Figure S5. AAV5-CaMKIIα::ChR2(H134R)-EYFP expression pattern in corticothalamic and thalamocortical pathways. ChR2 is expressed in cell bodies located near the site of virus injection and throughout axonal fibers projecting from those cell bodies, but not expressed in cell bodies downstream from the site of injection, demonstrating under these conditions lack of axonal transduction. This is an important parameter to validate in each experimental preparation, as viruses (including some AAVs) can transduce axon terminals in certain circuits. We have found that for lentiviruses and for AAVs in cortical and corticothalamic circuits, among others, such axonal transduction is negligible; for example, in the case of animals with ChR2 injection into motor cortex, we observed no definitive cases of downstream labeled cell bodies despite confocal inspection of 1,253 cells within the corresponding region of the thalamus, and only 6 of these 1,253 were even equivocal within the limits of the microscopy. Confocal images of brain slices from **a**, motor cortex, **b**, striatum, and **c**, thalamus for animals with virus injection in motor cortex (left) and thalamus (right). ChR2 expression is localized to neurons with cell bodies at the viral injection sites, as shown in **a** (*left*) and **c** (*right*) (arrows); costain is with DAPI (white) to identify nuclei.